

Hammer, Martin; Sauer, Lydia; Klemm, Matthias; Peters, Sven; Schultz, Rowena; Haueisen, Jens:

Fundus autofluorescence beyond lipofuscin: lesson learned from ex vivo fluorescence lifetime imaging in porcine eyes

Original published in:

Biomedical optics express. - Washington, DC : OSA. - 9 (2018), 7, p. 3078-3091.

Original published: July 01, 2018

ISSN: 2156-7085

DOI: [10.1364/BOE.9.003078](https://doi.org/10.1364/BOE.9.003078)

[Visited: July 08, 2019]

© 2018 Optical Society of America under the terms of the OSA Open Access Publishing Agreement.

[Licence URL: https://doi.org/10.1364/OA_License_v1]

Authors and readers may use, reuse, and build upon the article, or use it for text or data mining without asking prior permission from the publisher or the Author(s), as long as the purpose is non-commercial and appropriate attribution is maintained.



Fundus autofluorescence beyond lipofuscin: lesson learned from *ex vivo* fluorescence lifetime imaging in porcine eyes

MARTIN HAMMER,^{1,2,*} LYDIA SAUER,^{1,3} MATTHIAS KLEMM,⁴ SVEN PETERS,¹ ROWENA SCHULTZ,¹ AND JENS HAUEISEN⁴

¹University Hospital Jena, Department of Ophthalmology, 07747 Jena, Am Klinikum 1, Germany

²University of Jena, Center for Biomedical Optics and Photonics, 07740 Jena, Germany

³John A. Moran Eye Center, University of Utah, Salt Lake City, UT, USA

⁴Technical University Ilmenau, Institute for Biomedical Engineering and Informatics, Gustav-Kirchhoff-Str. 2, 98693 Ilmenau, Germany

*martin.hammer@med.uni-jena.de

Abstract: Fundus autofluorescence (FAF) imaging is a well-established method in ophthalmology; however, the fluorophores involved need more clarification. The FAF lifetimes of 20 post mortem porcine eyes were measured in two spectral channels using fluorescence lifetime imaging ophthalmoscopy (FLIO) and compared with clinical data from 44 healthy young subjects. The FAF intensity ratio of the short and the long wavelength emission (spectral ratio) was determined. *Ex vivo* porcine fundus fluorescence emission is generally less intense than that seen in human eyes. The porcine retina showed significantly ($p < 0.05$) longer lifetimes than the retinal pigment epithelium (RPE): 584 ± 128 ps vs. 121 ± 55 ps 498–560 nm, 240 ± 42 ps vs. 125 ± 20 ps at 560–720 nm. Furthermore, the lifetimes of the porcine RPE were significantly shorter (121 ± 55 ps and 125 ± 20 ps) than those measured from human fundus *in vivo* (162 ± 14 ps and 179 ± 13 ps, respectively). The fluorescence emission of porcine retina was shifted towards a shorter wavelength compared to that of RPE and human FAF. This data shows the considerable contribution of fluorophores in the neural retina to total FAF intensity in porcine eyes.

© 2018 Optical Society of America under the terms of the [OSA Open Access Publishing Agreement](#)

OCIS codes: (170.3650) Lifetime-based sensing; (170.0170) Medical optics and biotechnology; (170.3880) Medical and biological imaging; (170.4470) Ophthalmology; (170.6510) Spectroscopy, tissue diagnostics; (300.2530) Fluorescence, laser-induced.

References and links

1. F. C. Delori, C. K. Dorey, G. Staurenghi, O. Arend, D. G. Goger, and J. J. Weiter, "In vivo fluorescence of the ocular fundus exhibits retinal pigment epithelium lipofuscin characteristics," *Invest. Ophthalmol. Vis. Sci.* **36**(3), 718–729 (1995).
2. G. E. Eldred and M. L. Katz, "Fluorophores of the Human Retinal Pigment Epithelium - Separation and Spectral Characterization," *Exp. Eye Res.* **47**(1), 71–86 (1988).
3. J. P. Greenberg, T. Duncker, R. L. Woods, R. T. Smith, J. R. Sparrow, and F. C. Delori, "Quantitative fundus autofluorescence in healthy eyes," *Invest. Ophthalmol. Vis. Sci.* **54**(8), 5684–5693 (2013).
4. W. Einbock, A. Moessner, U. E. Schnurrbusch, F. G. Holz, and S. Wolf, "Changes in fundus autofluorescence in patients with age-related maculopathy. Correlation to visual function: a prospective study," *Graefes Arch. Clin. Exp. Ophthalmol.* **243**(4), 300–305 (2005).
5. S. Schmitz-Valckenberg, A. Bindewald-Wittich, J. Dolar-Szczasny, J. Dreyhaupt, S. Wolf, H. P. Scholl, and F. G. Holz, "Correlation between the area of increased autofluorescence surrounding geographic atrophy and disease progression in patients with AMD," *Invest. Ophthalmol. Vis. Sci.* **47**(6), 2648–2654 (2006).
6. S. Schmitz-Valckenberg, F. G. Holz, A. C. Bird, and R. F. Spaide, "Fundus autofluorescence imaging: review and perspectives," *Retina* **28**(3), 385–409 (2008).
7. F. C. Delori, M. R. Fleckner, D. G. Goger, J. J. Weiter, and C. K. Dorey, "Autofluorescence distribution associated with drusen in age-related macular degeneration," *Invest. Ophthalmol. Vis. Sci.* **41**(2), 496–504 (2000).
8. T. Ben Ami, Y. Tong, A. Bhuiyan, C. Huisin, Z. Ablonczy, T. Ach, C. A. Curcio, and R. T. Smith, "Spatial and Spectral Characterization of Human Retinal Pigment Epithelium Fluorophore Families by *Ex Vivo* Hyperspectral Autofluorescence Imaging," *Transl. Vis. Sci. Technol.* **5**(3), 5 (2016).

9. D. Schweitzer, E. R. Gaillard, J. Dillon, R. F. Mullins, S. Russell, B. Hoffmann, S. Peters, M. Hammer, and C. Biskup, "Time-resolved autofluorescence imaging of human donor retina tissue from donors with significant extramacular drusen," *Invest. Ophthalmol. Vis. Sci.* **53**(7), 3376–3386 (2012).
10. U. Kellner, S. Kellner, and S. Weinitz, "Fundus autofluorescence (488 NM) and near-infrared autofluorescence (787 NM) visualize different retinal pigment epithelium alterations in patients with age-related macular degeneration," *Retina* **30**(1), 6–15 (2010).
11. M. B. Parodi, P. Iacono, C. Del Turco, and F. Bandello, "Near-infrared fundus autofluorescence in subclinical best vitelliform macular dystrophy," *Am. J. Ophthalmol.* **158**(6), 1247–1252.e2 (2014).
12. T. Ueda-Consolvo, A. Miyakoshi, H. Ozaki, S. Houki, and A. Hayashi, "Near-infrared fundus autofluorescence-visualized melanin in the choroidal abnormalities of neurofibromatosis type 1," *Clin. Ophthalmol.* **6**, 1191–1194 (2012).
13. R. Spaide, "Autofluorescence from the outer retina and subretinal space: hypothesis and review," *Retina* **28**(1), 5–35 (2008).
14. W. Becker, "Fluorescence lifetime imaging--techniques and applications," *J. Microsc.* **247**(2), 119–136 (2012).
15. D. Schweitzer, M. Hammer, F. Schweitzer, R. Anders, T. Doebbecke, S. Schenke, E. R. Gaillard, and E. R. Gaillard, "*In vivo* measurement of time-resolved autofluorescence at the human fundus," *J. Biomed. Opt.* **9**(6), 1214–1222 (2004).
16. D. Schweitzer, A. Kolb, and M. Hammer, "Autofluorescence lifetime measurements in images of the human ocular fundus," *Proc. SPIE* **4432**, 29–39 (2001).
17. D. Schweitzer, S. Schenke, M. Hammer, F. Schweitzer, S. Jentsch, E. Birckner, W. Becker, and A. Bergmann, "Towards metabolic mapping of the human retina," *Microsc. Res. Tech.* **70**(5), 410–419 (2007).
18. C. Dysli, G. Quellec, M. Abegg, M. N. Menke, U. Wolf-Schnurrbusch, J. Kowal, J. Blatz, O. La Schiazza, A. B. Leichtle, S. Wolf, and M. S. Zinkernagel, "Quantitative analysis of fluorescence lifetime measurements of the macula using the fluorescence lifetime imaging ophthalmoscope in healthy subjects," *Invest. Ophthalmol. Vis. Sci.* **55**(4), 2106–2113 (2014).
19. L. Sauer, D. Schweitzer, L. Ramm, R. Augsten, M. Hammer, and S. Peters, "Impact of Macular Pigment on Fundus Autofluorescence Lifetimes," *Invest. Ophthalmol. Vis. Sci.* **56**(8), 4668–4679 (2015).
20. L. Sauer, S. Peters, J. Schmidt, D. Schweitzer, M. Klemm, L. Ramm, R. Augsten, and M. Hammer, "Monitoring Macular Pigment changes in Macular Holes using Fluorescence Lifetime Imaging Ophthalmoscopy (FLIO)," *Acta ophthalmologica* **95**(5), 481–492 (2016).
21. D. M. Ciobanu, L. E. Olar, R. Stefan, I. A. Veresiu, C. G. Bala, P. A. Mircea, and G. Roman, "Fluorophores advanced glycation end products (AGEs)-to-NADH ratio is predictor for diabetic chronic kidney and cardiovascular disease," *J. Diabetes Complications* **29**(7), 893–897 (2015).
22. J. Schmidt, S. Peters, L. Sauer, D. Schweitzer, M. Klemm, R. Augsten, N. Muller, and M. Hammer, "Fundus autofluorescence lifetimes are increased in non-proliferative diabetic retinopathy," *Acta Ophthalmol.* **95**(1), 33–40 (2017).
23. D. Schweitzer, L. Deutsch, M. Klemm, S. Jentsch, M. Hammer, S. Peters, J. Haueisen, U. A. Muller, and J. Dawczynski, "Fluorescence lifetime imaging ophthalmoscopy in type 2 diabetic patients who have no signs of diabetic retinopathy," *J Biomed Opt* **20**, 61106 (2015).
24. L. Sauer, "Fluorescence Lifetime Imaging Ophthalmoscopy (FLIO) - a novel way to assess changes in MacTel," in *Lowy Medical Research Institute (LMRI) annual meeting* (New York City, 2017).
25. C. Dysli, S. Wolf, K. Hatz, and M. S. Zinkernagel, "Fluorescence Lifetime Imaging in Stargardt Disease: Potential Marker for Disease Progression," *Invest. Ophthalmol. Vis. Sci.* **57**(3), 832–841 (2016).
26. C. Dysli, S. Wolf, H. V. Tran, and M. S. Zinkernagel, "Autofluorescence Lifetimes in Patients With Choroideremia Identify Photoreceptors in Areas With Retinal Pigment Epithelium Atrophy," *Invest. Ophthalmol. Vis. Sci.* **57**(15), 6714–6721 (2016).
27. C. Dysli, L. Berger, S. Wolf, and M. S. Zinkernagel, "Fundus Autofluorescence Lifetimes and Central Serous Chorioretinopathy," *Retina* **37**(11), 2151–2161 (2017).
28. D. Schweitzer, L. Deutsch, M. Klemm, S. Jentsch, M. Hammer, S. Peters, J. Haueisen, U. A. Müller, and J. Dawczynski, "Fluorescence lifetime imaging ophthalmoscopy in type 2 diabetic patients who have no signs of diabetic retinopathy," *J. Biomed. Opt.* **20**(6), 061106 (2015).
29. J. H. Prince, C. D. Diesem, I. Eglitis, and G. L. Ruskell, *Anatomy and Histology of the Eye and Orbit in Domestic Animals* (Charles C. Thomas, 1965).
30. C. Dysli, S. Wolf, M. Y. Berezin, L. Sauer, M. Hammer, and M. S. Zinkernagel, "Fluorescence lifetime imaging ophthalmoscopy," *Prog. Retin. Eye Res.* **60**, 120–143 (2017).
31. W. Becker, A. Bergmann, M. A. Hink, K. König, K. Benndorf, and C. Biskup, "Fluorescence lifetime imaging by time-correlated single-photon counting," *Microsc. Res. Tech.* **63**(1), 58–66 (2004).
32. M. Klemm, D. Schweitzer, S. Peters, L. Sauer, M. Hammer, and J. Haueisen, "FLIMX: A Software Package to Determine and Analyze the Fluorescence Lifetime in Time-Resolved Fluorescence Data from the Human Eye," *PLoS One* **10**(7), e0131640 (2015).
33. M. Gloesmann, B. Hermann, C. Schubert, H. Sattmann, P. K. Ahnelt, and W. Drexler, "Histologic correlation of pig retina radial stratification with ultrahigh-resolution optical coherence tomography," *Invest. Ophthalmol. Vis. Sci.* **44**(4), 1696–1703 (2003).

34. F. Schütt, M. Bergmann, F. G. Holz, and J. Kopitz, "Isolation of intact lysosomes from human RPE cells and effects of A2-E on the integrity of the lysosomal and other cellular membranes," *Graefes Arch. Clin. Exp. Ophthalmol.* **240**(12), 983–988 (2002).
35. C. N. Keilhauer and F. C. Delori, "Near-infrared autofluorescence imaging of the fundus: visualization of ocular melanin," *Invest. Ophthalmol. Vis. Sci.* **47**(8), 3556–3564 (2006).
36. A. Ehlers, I. Riemann, M. Stark, and K. König, "Multiphoton fluorescence lifetime imaging of human hair," *Microsc. Res. Tech.* **70**(2), 154–161 (2007).
37. E. Dimitrow, I. Riemann, A. Ehlers, M. J. Koehler, J. Norgauer, P. Elsner, K. König, and M. Kaatz, "Spectral fluorescence lifetime detection and selective melanin imaging by multiphoton laser tomography for melanoma diagnosis," *Exp. Dermatol.* **18**(6), 509–515 (2009).
38. S. Peters, M. Hammer, and D. Schweitzer, "Two-photon excited fluorescence microscopy application for *ex vivo* investigation of ocular fundus samples," in ECBO, P. T. C. So, and E. Beaufort, eds. (SPIE, Munich, Germany, 2011), pp. 808605–808610.
39. M. Y. Loguinova, V. E. Zagidullin, T. B. Feldman, Y. V. Rostovtseva, V. Z. Paschenko, A. B. Rubin, and A. A. Ostrovsky, "Spectral Characteristics of Fluorophores Formed via Interaction between All-trans-Retinal with Rhodopsin and Lipids in Photoreceptor Membrane of Retina Rod Outer Segments," *Biochem. Moscow Suppl. Ser. A* **26**, 83–93 (2009).
40. J. J. Hunter, B. Masella, A. Dubra, R. Sharma, L. Yin, W. H. Merigan, G. Palczewska, K. Palczewski, and D. R. Williams, "Images of photoreceptors in living primate eyes using adaptive optics two-photon ophthalmoscopy," *Biomed. Opt. Express* **2**(1), 139–148 (2011).
41. R. Sharma, C. Schwarz, J. J. Hunter, G. Palczewska, K. Palczewski, and D. R. Williams, "Formation and Clearance of All-Trans-Retinal in Rods Investigated in the Living Primate Eye With Two-Photon Ophthalmoscopy," *Invest. Ophthalmol. Vis. Sci.* **58**(1), 604–613 (2017).
42. C. Chen, E. Tsina, M. C. Cornwall, R. K. Crouch, S. Vijayaraghavan, and Y. Koutalos, "Reduction of all-trans retinal to all-trans retinol in the outer segments of frog and mouse rod photoreceptors," *Biophys. J.* **88**(3), 2278–2287 (2005).
43. M. Garcá, J. Ruiz-Ederra, H. Hernández-Barbáchano, and E. Vecino, "Topography of pig retinal ganglion cells," *J. Comp. Neurol.* **486**(4), 361–372 (2005).
44. R. T. Smith, M. A. Sohrab, M. Busuioac, and G. Barile, "Reticular macular disease," *Am. J. Ophthalmol.* **148**(5), 733–743.e2 (2009).
45. M. C. Skala, K. M. Ricking, A. Gendron-Fitzpatrick, J. Eickhoff, K. W. Eliceiri, J. G. White, and N. Ramanujam, "*In vivo* multiphoton microscopy of NADH and FAD redox states, fluorescence lifetimes, and cellular morphology in precancerous epithelia," *Proc. Natl. Acad. Sci. U.S.A.* **104**(49), 19494–19499 (2007).
46. C. Dysli, M. Dysli, V. Enzmann, S. Wolf, and M. S. Zinkernagel, "Fluorescence lifetime imaging of the ocular fundus in mice," *Invest. Ophthalmol. Vis. Sci.* **55**(11), 7206–7215 (2014).
47. D. Schweitzer, M. Klemm, S. Quick, L. Deutsch, S. Jentsch, M. Hammer, J. Dawczynski, C. H. Kloos, and U. A. Mueller, "Detection of early metabolic alterations in the ocular fundus of diabetic patients by time-resolved autofluorescence of endogenous fluorophores," *Proc. SPIE* **8087**, 80871G (2011).
48. J. Burd, S. Lum, F. Cahn, and K. Ignatz, "Simultaneous noninvasive clinical measurement of lens autofluorescence and rayleigh scattering using a fluorescence biomicroscope," *J. Diabetes Sci. Technol.* **6**(6), 1251–1259 (2012).
49. J. Chen, P. R. Callis, and J. King, "Mechanism of the very efficient quenching of tryptophan fluorescence in human gamma D- and gamma S-crystallins: the gamma-crystallin fold may have evolved to protect tryptophan residues from ultraviolet photodamage," *Biochemistry* **48**(17), 3708–3716 (2009).
50. P. Garcia-Barreno, M. C. Guisasola, and A. Suarez, "Fluorescent and compositional changes in crystallin supramolecular structures in pig lens during development," *Comp. Biochem. Physiol. B Biochem. Mol. Biol.* **141**(2), 179–185 (2005).
51. A. Batista, H. G. Breunig, A. Uchugonova, A. M. Morgado, and K. König, "Two-photon spectral fluorescence lifetime and second-harmonic generation imaging of the porcine cornea with a 12-femtosecond laser microscope," *J. Biomed. Opt.* **21**(3), 036002 (2016).
52. M. L. Beauchemin, "The fine structure of the pig's retina," *Albrecht Von Graefes Arch. Klin. Exp. Ophthalmol.* **190**(1), 27–45 (1974).
53. T. I. Chao, J. Grosche, K. J. Friedrich, B. Biedermann, M. Francke, T. Pannicke, W. Reichelt, M. Wulst, C. Mühle, S. Pritz-Hohmeier, H. Kuhrt, F. Faude, W. Drommer, M. Kasper, E. Buse, and A. Reichenbach, "Comparative studies on mammalian Müller (retinal glial) cells," *J. Neurocytol.* **26**(7), 439–454 (1997).
54. A. Hendrickson and D. Hicks, "Distribution and density of medium- and short-wavelength selective cones in the domestic pig retina," *Exp. Eye Res.* **74**(4), 435–444 (2002).

1. Introduction

In recent years, fundus autofluorescence (FAF) intensity imaging has been established as diagnostic technique in clinical ophthalmology. Generally, fluorescence excited at wavelengths in the visible spectral range is assumed to be emitted by lipofuscin [1]. Lipofuscin is a mixture of various metabolic byproducts, predominantly all-trans retinal

derived compounds as well as lipid peroxidation products, accumulated in the lysosomes of the retinal pigment epithelium (RPE) [2]. This accumulation is age-dependent and might be involved in the pathogenesis of age-related macular degeneration (AMD) [3]. Thus, FAF is widely used to characterize the progression of AMD and other retinal dystrophies [4–7].

However, the application of autofluorescence in ophthalmology goes beyond simply monitoring lipofuscin. Spectrally resolved autofluorescence measurements in human donor eyes provides evidence for the spectral, and thus chemical, diversity of naturally occurring fluorophores in the human retina, healthy or affected with AMD [8]. This study as well as the spectrometric and autofluorescence lifetime investigation in AMD donor eyes by our group reveal differences between the lipofuscin contents in drusen versus RPE [9]. Furthermore, infrared-induced autofluorescence has been used to highlight the melanin in the RPE and might contribute to clinical diagnostics in various retinal diseases [10–12]. Spaide investigated autofluorescent compounds in the outer retina and the sub-retinal space with a fundus camera equipped with a specific filter set to all-trans-retinal-derived compounds, such as the pyridinium bis-retinoid A2E, its precursor products A2-PE and A2-PE-H2, and all-trans retinal dimers. These subretinal accumulations are a result of lacking phagocytosis by the RPE. The hereby investigated retinal diseases showed alterations that cannot solely be explained by lipofuscin fluorescence [13]. Thus, an investigation of non-lipofuscin compounds that contribute to FAF is of eminent diagnostic interest.

Fluorescence lifetime imaging ophthalmoscopy (FLIO) is a technique that measures the decay of fluorescence over time. It is used to characterize fluorophores, as well as their interaction with each other or the embedding matrix [14]. We introduced the technique of fluorescence lifetime imaging to the eye by using laser scanning ophthalmoscopy (SLO) [15–17]. FLIO shows an age-dependency for fluorescence lifetimes which is suggested to be a change in the lipofuscin composition with aging [18]. Furthermore, we found that the macular pigment contributed to FAF [19, 20]. In diabetic retinopathy, a prolongation in fluorescence lifetimes was found, pointing to the autofluorescence contribution of glycated proteins, which are known to be fluorescent [21–23]. FLIO already detects changes in retinal diseases at early stages [24–28]. Besides lipofuscin, melanin, collagen, elastin, FAD, and eventually NAD(P)H way contribute to FAF. We reported the fluorescence characteristics as well as the abundance of these compounds elsewhere [9, 17]. In order to rightfully classify such changes, investigating non-lipofuscin compounds with FLIO will lead to a better understanding of the method. Furthermore, information about fluorescence components from within the neural retina is highly relevant as many retinal diseases go along with neuronal changes.

This study investigates the contribution of non-lipofuscin fluorophores to FAF intensity and lifetimes in porcine eyes. These were used because their fundus is similar to that of primates. Pigs do not have a tapetum and the retina resembles that of humans and is well populated with cones. Although they lack a fovea, pigs have a macula-like area free of retinal vessels at the posterior pole [29]. As those eyes were obtained from pigs, slaughtered at an age of about 6 months, they are expected to contain minor amounts of lipofuscin only and, thus, are suitable to study other fluorophores.

2. Methods

2.1. Porcine eye preparation and investigation

Eyes of six month old pigs were obtained from a local slaughterhouse, transported, and investigated within eight hours post mortem. Although 20 eyes were used in these experiments, some measurements were excluded for technical reasons (see below). Eyes were transported and stored in Dulbecco's modified Eagle's medium (Gibco, Grand Island, NY) at 6 °C until use. As described below, they were investigated in front of the FLIO device and also with optical coherence tomography (OCT; Cirrus, Zeiss Meditec, Jena, Germany) in the high definition mode. Subsequently, they were dissected in the following way: An incision was made 3 mm posterior to the pars plana and a circumferential cut was performed. The anterior

part of the eye was removed and the vitreous was carefully peeled off. A triangular segment was cut out from the eye cup. The retina was removed from half of the specimen in order to allow simultaneous measurements of both retina and RPE fluorescence. The tissue was placed in the focal plane of a model eye with a 20 mm focal length and positioned in front of the FLIO for the measurement. In the same way, the fluorescence decay of the lens was recorded by focusing the FLIO scanner onto the anterior part of the intact eye. Additionally, the retina of 15 eyes was carefully dissected from the RPE and placed in an air-tight sealed silica glass cuvette (Hellma Optics, Jena, Germany, path length: 0.2mm) under balanced salt solution. Fluorescence lifetimes and spectral ratios were measured as described above.

2.2. Fluorescence lifetime imaging

Fluorescence lifetimes were recorded using a Spectralis-based FLIO prototype device (Heidelberg Engineering GmbH, Heidelberg, Germany). The technique is described in detail elsewhere [15, 18, 19, 30]. Briefly, the fundus was scanned with a 256 x 256 pixel raster in a 30° field at a frame rate of 9 Hz. Fluorescence was excited by a pulsed diode laser at 473 nm (repetition rate 80 MHz). Fluorescence photons were counted into one of 1024 time channels according to their time delays from the excitation pulse (time-correlated single photon counting, TCSPC, Becker and Hickl GmbH, Berlin, Germany [31]). The minimal signal threshold was 1000 photons for each pixel. Fluorescence photons were recorded in two spectral channels, at short-wavelength (SSC, 498–560 nm) and long-wavelength (LSC, 560–720 nm) channels. These two channels are implemented in the device to account for different emission maxima of different fluorophores and enable a rough spectral characteristic of FAF (see below). FLIO allows for a time resolution of about 30 ps [19].

FLIO does not measure the absolute fluorescence intensities. However, because single fluorescence photons are counted, the time needed to record a fixed number of photons gives a rough estimate of the fluorescence strength. Because the rapid opacification of lens and cornea result in a decrease in fluorescence, only measurements within the first 2 h post-mortem were included in a semi-quantitative comparison of the fluorescence intensities. Fluorescence lifetimes, which are independent from fluorescence intensity, were measured between one and eight hours post-mortem. Furthermore, the ratio of the fluorescence intensity (i.e. number of fluorescence photons in the SSC versus that in the LSC - spectral ratio) was determined in order to estimate the spectral differences in the fluorescence emissions of the tissues. To compensate for the different sensitivities of the detectors, we performed a calibration using sodium fluorescein, which has a well-known emission spectrum upon excitation at 470 nm.

2.3. Two-photon microscopy

In order to check for lipofuscin granules, one porcine and one human donor eye RPE sample were fixated in 4% paraformaldehyde and examined by two-photon microscopy. A LSM 710 (Carl Zeiss, Jena, Germany), equipped with a titanium-sapphire femtosecond laser (Chameleon Ultra, Coherent Inc., Santa Clara, CA) and a 40x water immersion objective (NA = 1.0) was used. The laser wavelength was set to 760 nm and the same fluorescence lifetime detection technique as in the FLIO was used.

2.4. Data processing and analysis

Fluorescence decays were approximated with a three-exponential model, fitted to the decay measured in each pixel, using the software SPCImage (Becker and Hickl GmbH). The three-exponential model was chosen to be consistent with the analysis of clinical FLIO data and results in three decay times, three weighting factors for these time constants as well as the amplitude-weighted mean autofluorescence lifetime τ_m . For the sake of the signal-to-noise ratio, a sliding average of 5 x 5 pixels was used for the fits. The software package FLIMX [32], which is documented and freely available for download online under the open source

BSD–license (<http://www.flimx.de>), was used to average τ_m over the regions of interest (ROI): the retina (excluding vessels) and the RPE. Separate calculations were performed for the two spectral channels. Because the autofluorescence lifetimes were relatively homogenous across the porcine fundus, retina, and RPE (except for optic disk and vessels), rectangular ROI with a minimal size of 544 square pixels were analyzed. The spectral ratio was determined in the same way. The means of the τ_m and spectral ratios were compared for different tissues (retina and RPE), defined by the ROIs, and measuring conditions (intact eye or preparation of the fundus) by ANOVA with post-hoc test using least significant differences (LSD, $p < 0.05$ was considered to be a significant difference) after the normal distribution of the data was confirmed by a Kolmogorow-Smirnow test. Furthermore, these data were analyzed with respect to their dependence on the post-mortem time by a correlation analysis. All of the statistical tests were conducted using SPSS (SPSS statistics 21, IBM Corp, Armonk, NY).

2.5. Human eyes

In order to compare our measurements from porcine samples with FAF lifetimes of human eyes *in vivo*, data from an earlier study was used with permission of the respective subjects [19]. Mean FAF lifetimes (τ_m) as well as spectral ratios at an eccentricity from 3mm to 5mm from the fovea were investigated from FLIO measurements of 44 healthy young subjects (mean age 24.1 ± 3.6 years).

3. Results

3.1. Porcine eyes

The retinal structure of the porcine eye is, except for the foveal pit, very similar to that of humans. To confirm that, OCT scans of the enucleated porcine eyes were performed. Figure 1 shows central (A) and peripheral (B) OCT scans approximately 1 h post mortem, as well as a peripheral (C) scan 7 h post mortem. Retinal scans as well as three-dimensional images of the scanned area further illustrate the mentioned similarities. Additionally, the different retinal layers, described by Gloesmann et al. [33], were marked in the peripheral scan 1 h post mortem. Although retinal structures are known to degenerate quickly, all of the layers appeared to be well-preserved 7 h post mortem on OCT scans.

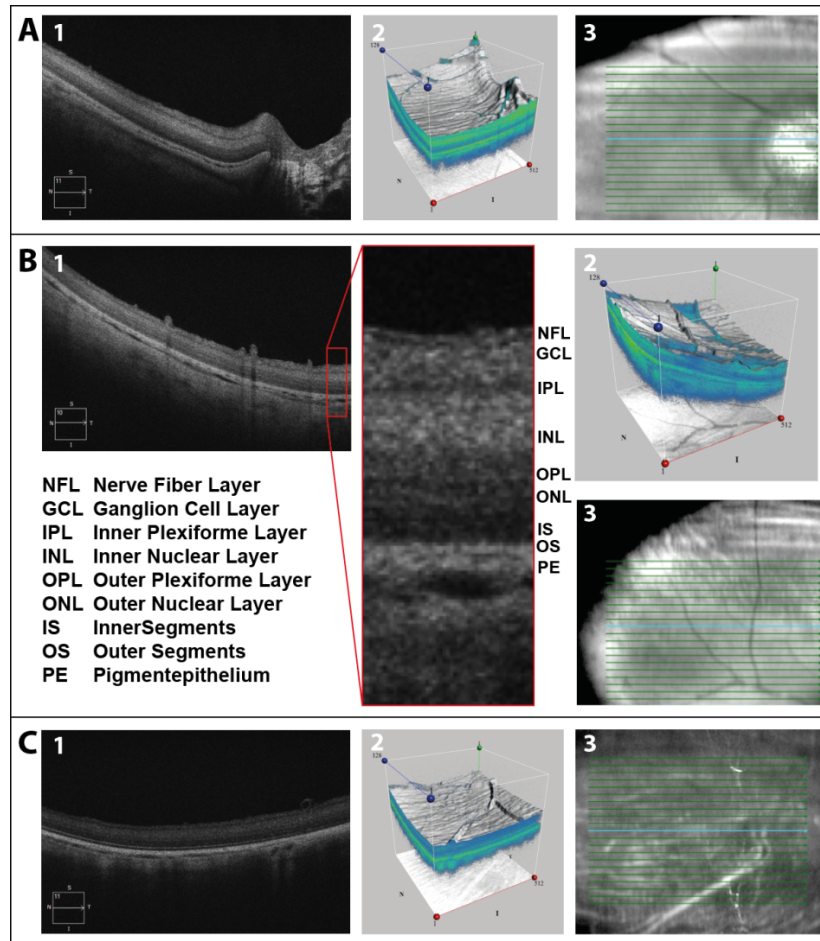


Fig. 1. Central (A) and peripheral (B) OCT-scan approximately 1 h post mortem, as well as peripheral (C) scan 7 h post mortem: (1) retinal scan, (2) three-dimensional image of scanned area, and (3) location of depicted scan. The different retinal layers were labeled in the peripheral scan 1 h post mortem. The blue line in the right column shows the scan position shown in the left column.

3.2. Porcine fundus fluorescence

The fluorescence characteristics in porcine eyes are presented in Fig. 2. Here, IR reflection, autofluorescence intensity, mean autofluorescence lifetime and spectral ratios are compared. The figure shows measurements from the fundus of the intact eye (1), the retina and RPE from the eye cup (2), and the lens (3). Because the specimen was curved, only the central part was in focus and provided a sufficient fluorescence signal, as shown in panels 2. Furthermore, two hyper-fluorescent spots with long lifetimes (indicated by the blue pseudo-color in panels 2C and 2D) show up, which are preparation artifacts with damages in the RPE, Bruch's membrane, and choroid.

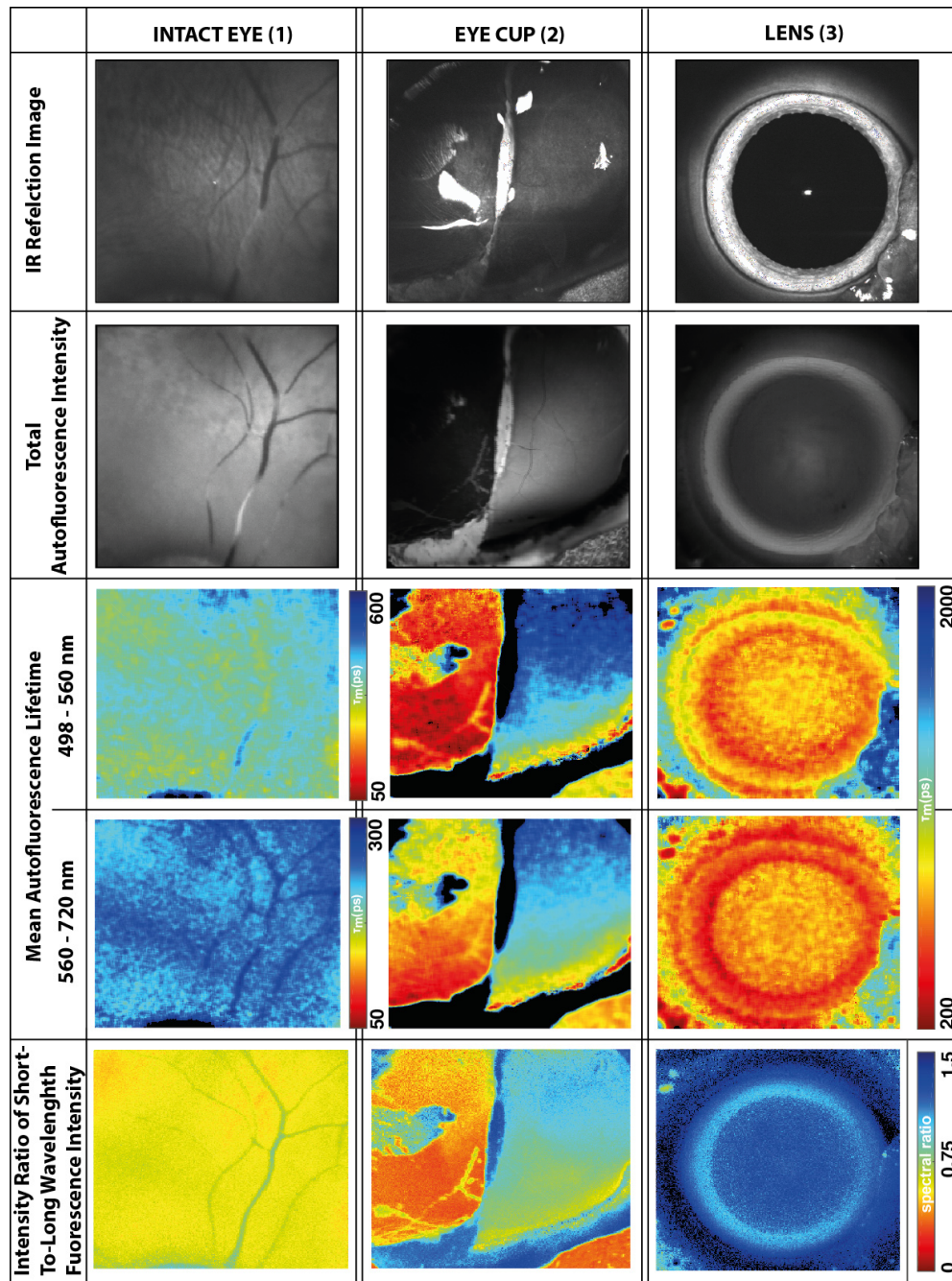


Fig. 2. Reflection and fluorescence images from retina in intact eye (1), retina and RPE of the eye cup (2) in focal plane of a model eye (i.e., without influences of anterior ocular media), and (3) lens. For the color-coding of the images, always refer to the nearest scale bar in the row. In the eye cup, the retina was removed in the left half. Thus, in panels 2, the right hand side shows the fluorescence of the retina, whereas at the left side shows that of the RPE.

The fluorescence from the *ex vivo* porcine fundus is generally less intense than that seen in human eyes. Although FLIO is not quantitative with respect to the fluorescence intensity, the strength of the fluorescence can be estimated from the time needed to record 1000 fluorescence photons per pixel. Whereas this took 2-3 minutes for the human retina in the

fovea, it needed 3-4 minutes for the porcine retina (intact eye). Furthermore, the fluorescence of the exposed RPE in the eye cup is even weaker. It took 8-10 minutes to reach the signal threshold in the exposed RPE part of the image. Because of an insufficient number of photons in the scans we had to exclude some measurements from further analysis (two measurements from the non-dissected fundus, one from the dissected retina and three from the dissected RPE of the porcine eyes).

The FAF lifetimes of the *ex vivo* porcine eyes were longer than that of the human cohort *in vivo*. The retina showed much higher fluorescence intensity (SSC: 7.7 ± 7.5 times, LSC: 3.4 ± 3.7 times) and longer lifetimes than the RPE in porcine eye cups. Data are shown in Table 1, and boxplots of the mean fluorescence lifetimes are presented graphically in Fig. 3. Also the isolated retina, measured in a sealed cuvette, showed considerable fluorescence. As it took about three minutes to collect 1000 photons, the fluorescence intensity was similar to that in the intact eye. Fluorescence lifetimes and spectral ratio are reported in Table 1.

Table 1. Mean fluorescence lifetime values τ_m at 498-560 nm and 560-720 nm as well as spectral ratio of the fluorescence emission intensity in both wavelength ranges. “Intact retina” and “RPE exposed” indicate data from the dissected eye cup whereas “isolated retina” denotes measurements at the retina dissected from RPE/choroid. “Human fundus” was measured *in vivo*

		mean	standard deviation	median	95% confidence interval
τ_m at 498-560nm [ps]	intact eye	389	39	386	369 - 409
	intact retina	584	128	593	523 - 646
	RPE exposed	121	55	110	93 - 149
	isolated retina	274	50	272	247 - 302
	human fundus	162	14	160	157 - 166
τ_m at 560-720nm [ps]	intact eye	237	22	238	226 - 248
	intact retina	240	42	244	220 - 261
	RPE exposed	125	20	117	115 - 136
	isolated retina	165	25	171	152 - 179
	human fundus	179	13	177	175 - 183
spectral ratio	intact eye	0.63	0.08	0.63	0.60 - 0.67
	intact retina	0.95	0.11	0.93	0.89 - 1.0
	RPE exposed	0.38	0.09	0.35	0.34 - 0.43
	isolated retina	0.63	0.06	0.61	0.59 - 0.66
	human fundus	0.42	0.05	0.43	0.41 - 0.44

In the SSC, the FAF lifetimes of porcine retina shifted to even longer means after the dissection of the eye. Only the autofluorescence lifetimes of the porcine RPE were shorter than that of the human *in vivo* FAF. The mean autofluorescence lifetimes were significantly different between the porcine fundus (intact eye), retina, and RPE (both dissected eye cup), and the human fundus in both spectral channels ($p < 0.05$ in ANOVA with LDS post hoc test), except for the difference between the porcine fundus of the intact eye and intact retina in the eye cup in the LSC.

We checked for changes in the autofluorescence over time post mortem. Although there seemed to be a slight decrease in fluorescence over time, no significant change in the lifetimes or spectral ratio over 8 h post mortem was found.

3.3. Spectral ratios

The spectral ratios of the fluorescence emission from the RPE as well as the human fundus were low. This indicates the dominance of the LSC (560–720 nm). The contribution of the fluorescence from the SSC (498–560 nm) was higher from the porcine fundus (intact eye) and the highest for the retina (dissected eye cup). All of the differences except those between the RPE and human fundus were statistically significant. Data are given in Table 1, and spectral ratios are shown in Fig. 4.

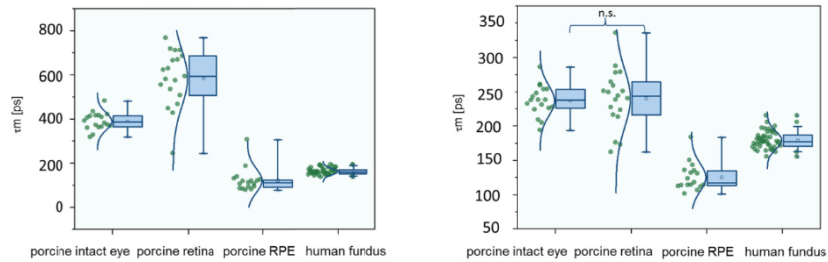


Fig. 3: Mean fluorescence lifetime values τ_m at 498-560 nm (left) and 560-720 nm (right). “Porcine retina” and “porcine RPE” indicate data from the dissected eye cup, “human fundus” was measured *in vivo*.

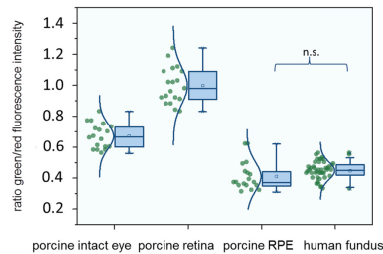


Fig. 4. Spectral ratio of fluorescence intensities at 498-560 nm and 560-720 nm.

3.4. Two-photon microscopy

Figure 5 shows fluorescence lifetime images of porcine and human RPE. As the human sample clearly shows the typical lipofuscin granules, the porcine RPE does not. Here, the fluorescence is more homogenous and fluorescence lifetimes are considerably shorter than in the lipofuscin granules in the human sample. This is in agreement with the FLIO results, in which, however, the resolution is not sufficient to see individual cells and cell compartments.

3.5. Lens autofluorescence

The lens autofluorescence was investigated in 11 porcine eyes. Lenses show slightly more fluorescence in the SSC, with a spectral ratio of 1.178 ± 0.053 and the same autofluorescence lifetimes in both spectral channels (τ_m SSC: 816 ± 108 ps; LSC: 815 ± 95 ps). No correlations were found between the lens and fundus autofluorescence lifetimes and spectral ratios.

4. Discussion

Fluorescence lifetime imaging ophthalmoscopy (FLIO) is a novel methodology to image the human retina *in vivo*. Alterations of FAF lifetimes were found in early stages of diseases, therefore the interest in this novel method is rising. However, a distinct attribution from changes to specific retinal fluorophores is still difficult. A large part of the fluorescence from the fundus can be assigned to lipofuscin [1]. The medium-long FAF lifetimes, found across

the human retina in a homogenous manner, was attributed to lipofuscin [24, 25, 30]. Additionally, we previously were able to characterize macular carotenoids as further retinal fluorophores impacting FLIO [19, 20]. Obviously, more than only those two fluorophores show an impact on FLIO from the human retina and RPE. Therefore, we propose a model to further investigate fluorophores other than lipofuscin by investigating *ex vivo* porcine eyes.

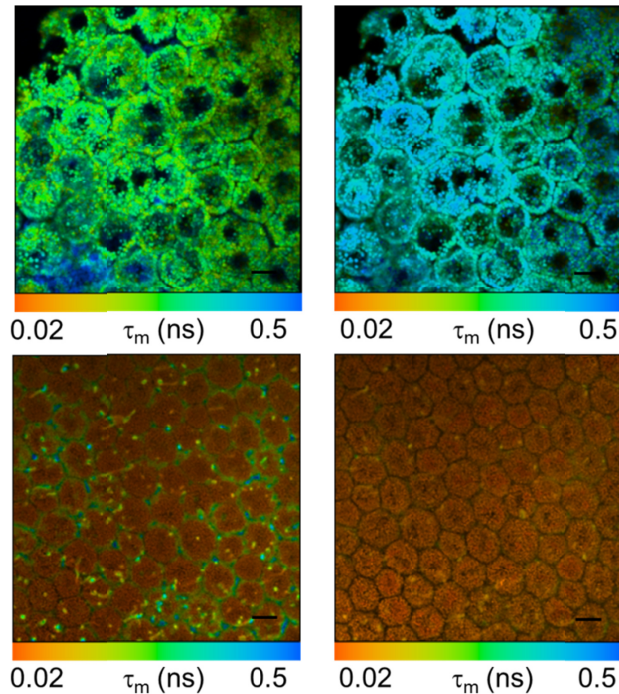


Fig. 5. Two-photon fluorescence lifetime micrographs of human (top) and porcine (bottom) RPE at emission bands 500-550nm (left) and 550-700nm (right). Scale bar: 10 μ m.

4.1. Fluorescence from the exposed RPE

Because the pigs were slaughtered at a young age, we expect the eyes to contain only small amounts of lipofuscin. This assumption is supported by the weak fluorescence of the RPE (Fig. 2, panel 2b) as lipofuscin is known to accumulate in RPE lysosomes [34]. Furthermore, two-photon microscopy (Fig. 5) did not show the presence of lipofuscin-containing granules in the porcine RPE. Therefore, the porcine eye appears to be a suitable model to study retinal or sub-retinal fluorophores other than lipofuscin. As the FAF in the investigated porcine eye cups shows higher intensity from the retina as compared to that of the RPE, and the isolated retina showed fluorescence intensities comparable to that of intact porcine eyes, retinal fluorophores has to be taken into account as well.

As the RPE lifetimes were short and showed no difference between spectral channels, we suppose that melanin could be the major fluorophore here. Melanin is assumed to dominate human FAF upon IR excitation with a fluorescence quantum yield one order of magnitude lower than that of lipofuscin [35]. Eumelanin, studied in human black hair, showed a predominant (> 80%) fluorescence decay component of 30 ps and a second one peaking at 800 ps [36]. Investigating melanocytes in human skin, nevi and melanomas, Dimitrow et al. found short lifetimes (205 ps) similar to those that we found in the RPE [37]. Similar short lifetimes were also found for the RPE using two-photon microscopy [38].

4.2. Fluorescence and possible fluorophores from within the neural retina in porcine and human eyes

While human FAF is attributed to all-trans-retinal (ATR)-derived compounds such as A2E and its precursor and oxidation products, ATR itself, which is highly concentrated in the retina, is basically non-fluorescent [39]. In this study the authors describe the accumulation of ATR derivatives formed in the process of interaction with amino groups of rhodopsin and with lipids by the incubation of rod outer segments membranes with a 10-fold excess of ATR over three days. In our study, we don't assume that ATR derivatives play a major role as both our experimental conditions as well as the FAF lifetimes that we found were different.

Also photoreceptors themselves cannot be excluded to impact the retinal autofluorescence. Hunter et al. demonstrated two-photon fluorescence in the macaque retina *in vivo* and *ex vivo* [40]. The photoreceptor fluorescence was found to be stronger after bleaching of the visual pigments. The kinetics of fluorescence changes after the onset of the two-photon imaging as well as after a visible light bleaching stimulus indicate the observation of the reduction of ATR to retinol and its subsequent clearance [41]. Retinol is known to be fluorescent only if excited at wavelengths below 400 nm [42]. As in our experiments, however, light of a wavelength far above 400 nm was used, we don't expect to see retinol fluorescence. Porcine eyes are known to possess a visual streak which is a region of high density of retinal ganglion cells [43]. In our data, we looked carefully on altered fluorescence lifetimes as a sign for a greater metabolic activity in this region, but didn't find any differences.

Ben Ami and colleagues found different fluorophore species using hyperspectral imaging in the RPE and Bruch's membrane of human donor eyes, which they attributed to different lipofuscin and melano-lipofuscin compounds [8]. However, because we only saw very weak RPE fluorescence in our porcine specimens, we do not think that these compounds contribute much to the fluorescence intensity seen here. We further exclude subretinal drusenoid deposits [44] as a source of fluorescence because we did not see any drusen in OCT.

Retinal fluorescence in the intact porcine eye was shifted towards shorter wavelengths as compared to human FAF. However, the SSC fluorescence changed in contrast to the LSC when we opened the globe and exposed the retina to oxygen. That hints that flavin adenine dinucleotide (FAD) might be a major retinal fluorophore. This ubiquitous co-enzyme of cellular energy metabolism was described with an autofluorescence lifetime of 2300 ps, which is quenched to 100 ps if it is bound to protein [17, 45]. Thus, the retinal lifetimes measured in the eye cup may indicate a mixture of both forms and a shift toward the free form in the case of an excess of oxygen. Accordingly, we found much shorter lifetimes in the isolated retina measured in air-sealed cuvettes. This is in agreement with findings from the two-photon excited measurement of the fluorescence spectra and lifetimes for single retinal layers [38]. The fluorescence spectra, measured in that paper upon excitation at 760 nm, clearly indicate the fluorescence of FAD and, predominantly, nicotinamide adenine dinucleotide (NADH). In contrast to that study, at 473 nm we predominantly excite FAD and little, if any, NADH.

The longer lifetimes in the SSC were consistent with the findings in mice *in vivo* using the same FLIO technique by Dysli et al. [46]. The shortening of the lifetimes with age in this study might indicate an increase in the contribution of lipofuscin. However, that study also gave no conclusive statement on the origin of the long lifetimes in young mice. Taken together the results from our study, supported by the findings of Dysli et al., indicate that there must be at least one more fluorophore that we have not yet discovered.

4.3. Lens autofluorescence

As is known from an investigation involving phakic and pseudophakic patients, the lens has an influence on the lifetimes measured from the human fundus [47]. Although the confocal optics of the Spectralis scanner greatly suppresses light (reflection, backscattering, and

fluorescence) from the lens, the human lens fluorescence is not completely blocked by the confocality. The porcine lens fluorescence seems to be weaker than that of the human lens. Thus, its influence on the FAF lifetimes might be minor, which is supported by the missing correlation between the lens and τ_m of the fundus.

The major sources of fluorescence in the crystallin lens are assumed to be tryptophan and advanced glycation end products (AGE) [22]. AGE accumulation [48] and less efficient fluorescence quenching [49] may contribute to changes in the fluorescence properties of a lens over its lifespan. As lens fluorescence is known to increase with age and cataract (unpublished data), the young age of the pigs used in this study may be the reason for the lower lens fluorescence and shorter FAF lifetimes compared to humans. This is in agreement with a change in the ratio of tryptophan and non-tryptophan fluorescence values in porcine lenses with age [50]. Additionally, fluorescence from the cornea [51] might contribute to the lens measurement. As, however, the cornea is out of the confocal plane, this influence is considered to be rather small.

4.4. Limitations

Although the retina of the domestic pig shows a very similar structure to that of a human (Fig. 1), it has no macula [52]. Additionally, the nerve fiber layer appears to be thicker in porcine eyes, and Mueller cells were found to reach only to the nerve fiber layer [53, 54]. Nevertheless, domestic pigs are similar to humans as they are able to view colors and their retinæ are not only compromised of rods, but also a large number of M- and S-cones [54]. This makes porcine eyes an eligible model for comparison to human eyes.

Secondly, the porcine eyes were investigated post mortem, whereas human eyes were investigated *in vivo*. Although post mortem times were short, the porcine eyes do not entirely show physiological conditions comparable to human eyes. It has to be noted that we don't know about the impact of death on fluorescence characteristics. The fluorophores might have changed in their composition and conformation, as compared to *in vivo* situations. However, as neither the fluorescence lifetimes nor the spectral ratio was found to change over time, we believe that changes might be minor. The reduction of the fluorescence intensity over the post mortem time was attributed to light loss by scattering because of anterior media opacification. Generally, it has to be noted that lens and cornea have a wavelength-dependent absorption and scattering which suppress short-wave fluorescence light from the fundus. This might have reduced the spectral ratio in the intact eye, however it should not have influenced the fluorescence lifetimes which are independent from the fluorescence intensities.

Furthermore, we assumed to only investigate the fluorescence of the retina and RPE, because we did not see long fluorescence lifetimes from the collagen and elastin in the sclera and Bruch's membrane. We also assumed Melanin fluorescence from the choroid to be greatly shielded by the RPE. However, we cannot completely rule out fluorescence contributions from these tissues. Although we did not see lipofuscin fluorescence in the porcine eyes, it cannot completely be excluded, that there is a minor lipofuscin fluorescence which is shielded by that of melanin granules located apically in the RPE.

Finally, we did not extract, purify, and identify the fluorophores because this was beyond the scope of the current investigation. Therefore, we can only make assumptions about the origin of the additional fluorophores which we detect.

5. Conclusion

We were able to show that non-lipofuscin fluorophores contributed to FAF when excited at 473 nm. Such fluorophores could be melanin or the co-enzymes of cellular energy metabolism, as for example FAD. Overall, our data suggests the presence of non-lipofuscin fluorophores, which possibly have to be taken into account in the interpretation of clinical FAF lifetimes of human eyes *in vivo* as well. The *ex vivo* porcine eye is a simple model to approach investigations on FAF lifetimes. Further investigations will be necessary to

elucidate to what extent these fluorophores contribute to the observation of clinical FAF intensity and lifetimes.

Funding

German Research Foundation, (HA 4430/3-1, Ha 2899/19-1); German Federal Ministry of Education and Research (03IPT605X).

Disclosure

The authors declare that there are no conflicts of interest related to this article.